



HAL
open science

N-glycosylation of the envelope glycoprotein I is essential for the proliferation and virulence of the duck plague virus

Yaru Ning, Mingshu Wang, Anchun Cheng, Qiao Yang, Bin Tian, Xumin Ou, Di Sun, Yu He, Zhen Wu, Xinxin Zhao, et al.

► **To cite this version:**

Yaru Ning, Mingshu Wang, Anchun Cheng, Qiao Yang, Bin Tian, et al.. N-glycosylation of the envelope glycoprotein I is essential for the proliferation and virulence of the duck plague virus. *Veterinary Research*, 2024, 55 (1), pp.139. 10.1186/s13567-024-01398-4 . hal-04755789

HAL Id: hal-04755789

<https://hal.science/hal-04755789v1>

Submitted on 28 Oct 2024

HAL is a multi-disciplinary open access archive for the deposit and dissemination of scientific research documents, whether they are published or not. The documents may come from teaching and research institutions in France or abroad, or from public or private research centers.


L'archive ouverte pluridisciplinaire **HAL**, est destinée au dépôt et à la diffusion de documents scientifiques de niveau recherche, publiés ou non, émanant des établissements d'enseignement et de recherche français ou étrangers, des laboratoires publics ou privés.

RESEARCH ARTICLE

Open Access



N-glycosylation of the envelope glycoprotein I is essential for the proliferation and virulence of the duck plague virus

Yaru Ning^{1,2,3†}, Mingshu Wang^{1,2,3,4,5†}, Anchun Cheng^{1,2,3,4,5*} , Qiao Yang^{1,2,3,4,5}, Bin Tian^{1,3,4,5}, Xumin Ou^{1,2,3,4,5}, Di Sun^{1,2,3,4,5}, Yu He^{1,2,3,4,5}, Zhen Wu^{1,2,3,4,5}, Xinxin Zhao^{1,2,3,4,5}, Shaqiu Zhang^{1,2,3,4,5}, Ying Wu^{1,2,3,4,5}, Juan Huang^{1,2,3,4,5}, Yanling Yu^{1,2,3}, Ling Zhang^{1,2,3}, Renyong Jia^{1,2,3,4,5}, Mafeng Liu^{1,2,3,4,5}, Dekang Zhu^{2,3,4,5} and Shun Chen^{1,2,3,4,5}

Abstract

Duck plague virus (DPV) causes the highly pathogenic duck plague, and the envelope glycoprotein I (gI), as one of the key virulence genes, has not yet had its critical virulence sites identified through screening. This study used reverse genetics technology to target the gI, specifically within the DPV genome. Four DPV mutants with gI N-glycosylation site mutations were designed and constructed, and these mutant strains were successfully rescued. Our results confirmed that three asparagine residues of gI (N₆₉, N₇₈, and N₂₆₅) are N-glycosylation sites, and western blot analysis substantiated that glycosylation at each predicted N-glycosylation site was compromised. The deglycosylation of gI leads to the protein misfolding and subsequent retention in the endoplasmic reticulum (ER). The subsequent deglycosylated gI is carried into the Golgi apparatus (GM130) in the interaction of gE. Compared to the parental virus, the mutated virus shows a 66.3% reduction in intercellular transmission capability. In ducks, the deglycosylation of gI significantly reduces DPV replication in vivo, thereby weakening the virulence of DPV. This study represents the first successful creation of a weak DPV virus strain by specific mutation at the N-glycosylation site. The findings provide a foundational understanding of DPV pathogenesis and form the basis for developing live attenuated vaccines against the disease.

Keywords Duck plague virus, virulence gene, glycoprotein I, N-glycosylation, pathogenicity

Handling editor: Stéphane Biacchesi

[†]Yaru Ning and Mingshu Wang contributed equally to this work. Author order depended on the degree of responsibility for the article.

*Correspondence:

Anchun Cheng
chenganchun@vip.163.com

¹ Institute of Veterinary Medicine and Immunology, Sichuan Agricultural University, Chengdu 611130, China

² Research Center of Avian Disease, College of Veterinary Medicine, Sichuan Agricultural University, Chengdu 611130, China

³ Key Laboratory of Animal Disease and Human Health of Sichuan Province, Chengdu 611130, China

⁴ International Joint Research Center for Animal Disease Prevention and Control of Sichuan Province, Chengdu 611130, China

⁵ Engineering Research Center of Southwest Animal Disease Prevention and Control Technology, Ministry of Education of the People's Republic of China, Chengdu 611130, China



© The Author(s) 2024. **Open Access** This article is licensed under a Creative Commons Attribution 4.0 International License, which permits use, sharing, adaptation, distribution and reproduction in any medium or format, as long as you give appropriate credit to the original author(s) and the source, provide a link to the Creative Commons licence, and indicate if changes were made. The images or other third party material in this article are included in the article's Creative Commons licence, unless indicated otherwise in a credit line to the material. If material is not included in the article's Creative Commons licence and your intended use is not permitted by statutory regulation or exceeds the permitted use, you will need to obtain permission directly from the copyright holder. To view a copy of this licence, visit <http://creativecommons.org/licenses/by/4.0/>. The Creative Commons Public Domain Dedication waiver (<http://creativecommons.org/publicdomain/zero/1.0/>) applies to the data made available in this article, unless otherwise stated in a credit line to the data.

Introduction

Duck plague (DP), also known as duck viral enteritis (DVE) [1], is an acute and highly contagious septicaemic disease. It is characterised by vascular damage, tissue haemorrhage, erosion of the gastrointestinal mucosa, impairment of lymphoid organs, and degenerative changes in solid organs. This disease affects ducks, geese, and other Anseriformes and is caused by duck plague virus (DPV) [2, 3]. China produces over 4 billion ducks annually, accounting for approximately 70% of the global output. DP is one of the most destructive diseases for the global waterfowl breeding industry, affecting many species. The incidence and mortality rates of DP can reach up to 95%, leading to significant economic losses and severely impacting the healthy development of the waterfowl breeding sector [2, 4]. Immunosuppression and latent infections resulting from DPV infection complicate prevention and control strategies that are used for the disease [5–7].

DPV belongs to the order *Herpesvirales*, family *Herpesviridae*, subfamily *Alphaherpesvirinae*, and genus *Marek's disease virus*. Mature DPV virions are spherical and relatively large, with a diameter ranging from 150 to 300 nm. The structure of DPV is complex, consisting of a core formed by the intertwining of double-stranded DNA and nucleoproteins, an icosahedral capsid structure made of proteins, a tegument layer also composed of proteins, and an outer envelope containing glycoproteins. The DPV CHv strain is a highly virulent virus with a genomic full length of 162 175 base pairs (bp), which includes 78 potential open reading frames (ORFs) encoding functional proteins [8]. The genomic structure consists primarily of a long unique region (UL), a short unique region (US), and internal repeats (IR) that flank the US region. The genome is arranged as 5'-UL-IRS-US-TRS-3'. In DPV research, multiple genes encoding envelope proteins have been identified. These envelope proteins are essential for the virus life cycle and pathogenicity. Specifically, the UL1, UL10, UL22, UL27, UL44, UL49.5, UL53, and US4-8 genes encode envelope proteins [9–12]. The envelope glycoprotein I (gI), encoded by the US7 gene, has been recognised as a crucial virulence factor for DPV. This finding was based on clinical symptom observations and gross pathological analysis of ducks infected with DPV Δ gI. Because of gI's significant role in viral pathogenicity, it has become a potential target for studying the mechanisms of viral attenuation [13, 14]. However, the molecular mechanisms by which gI is involved in DPV attenuation have not yet been reported. This indicates that there is still a knowledge gap in the field of DPV research.

Viral pathogens require the proper expression and localisation of virulence genes to ensure successful

infection. Like many proteins, virulence genes must undergo post-translational modifications to be correctly localised, secreted, and functional. N-glycosylation is a common post-translational modification that assists in the proper folding of newly synthesised proteins [15–17]. Proteins recognise polysaccharides through a specific consensus sequence N-X-T/S. Glycosyltransferases catalyse the attachment of polysaccharides to asparagine residues at specific sequences [18, 19]. Abnormal glycosylation can lead to reduced virulence in both animal and plant pathogens [20]. The Rotavirus (RV) non-structural protein 4 (NSP4) undergoes deglycosylation, which causes NSP4 to be mislocalised. This process leads to a delayed increase in cytosolic calcium ion concentration, a reduction in virus formation, and a significant decrease in the replication capacity of the glycosylation-deficient virus in various cell lines. This reduction ranges from 10 to 10 000-fold compared to the wild-type virus. Additionally, the pathogenicity of the glycosylation-deficient virus in mice is lower than that of the wild-type virus [21]. N-glycosylation modifications highly characterise the hemagglutinin (HA) protein of the influenza virus [22]. Removal of N-glycans from epitopes inhibits the recognition of HA by specific antibodies, thus helping the virus evade the host's humoral immune response [23, 24]. Typically, viruses increase their virulence by manipulating or evading the host's immune response [25, 26]. Herpesvirus glycoproteins gB, gH, gD, gI, and gM are all connected via asparagine-linked glycosylation, which plays an essential role in their proper folding, transport, and immune evasion [9, 27–31]. However, the precise role of DPV gI in viral proliferation and virulence within its natural host requires further investigation.

In this study, we comprehensively evaluated the functionality of all potential N-glycosylation sites on the DPV gI. We showed that N-glycosylated gI plays a critical role in organelle transport. When gI is deglycosylated, it loses its ability to move within host cells. Additionally, deglycosylation of gI significantly reduced the intercellular spread of the mutant virus. In ducks, deglycosylation of gI notably decreases the replication of DPV in vivo.

Materials and methods

Cells and viruses

Duck embryonic fibroblasts (DEFs) were derived from nine-day-old duck embryos and stored in Eagle's Minimum Essential Medium (MEM) (Gibco, Shanghai, China) supplemented with 10% Newborn Bovine Serum (NBS) (Gibco, MD, USA). HEK293T cells are maintained in our laboratory and preserved in 1640 Medium (Gibco, Shanghai, China) containing 10% Foetal Bovine Serum (FBS) (Gibco, MD, USA). All cells were cultured at 37 °C with 5% CO₂. The Chinese strong strain DPV

CHv (GenBank login number: JQ647509) has been sequenced for 50 generations of cytotoxic DPV CHv₅₀ in DEFs. This strain was preserved and provided by the Institute of Immunology, College of Veterinary Medicine, Sichuan Agricultural University.

Plasmids

Recombinant plasmids were designed based on the eukaryotic vector pCAGGS. These plasmids include pCAGGS-gI-Flag, pCAGGS-gI_{N69A}-Flag, pCAGGS-gI_{N78A}-Flag, pCAGGS-gI_{N265A}-Flag, and pCAGGS-gI_{N69/78/265A}-Flag, for the expression of recombinant gI. In summary, the gI gene fragment was amplified from the DPV CHv strain, and a Flag tag was introduced at its C-terminus and cloned into the *EcoR* I and *Bgl* II restriction enzyme-linearised pCAGGS vector. Using the oligonucleotide primers shown in Table 1, different N-glycosylation site mutations were introduced into the gI gene by standard overlapping PCR.

Moreover, we have introduced the “Kan” fragment into the aforementioned five recombinant vectors to create infectious clones containing gI mutations. Using pCAGGS-gI-Flag as a model, we used the oligonucleotide primers listed in Table 1 to amplify the “Kan” fragment from the pEP-Kan-S vector. We then cloned this fragment into the *Bgl* II restriction enzyme-linearised pCAGGS-gI-Flag vector, creating the pCAGGS-gI-Flag-Kan recombinant plasmid.

Construction and rescue of recombinant viruses

The infectious clones pDPV CHvΔgI and pDPV CHvΔgI+ΔgE, which are deletions of the DPV CHv strain, were provided by our laboratory. These clones were used to create the following gI mutant infectious clones: pDPV CHv-gI_{N69A}, pDPV CHv-gI_{N78A}, pDPV CHv-gI_{N265A}, pDPV CHv-gI_{N69/78/265A}, pDPV CHv-gI_{N69/78/265A} repair, and pDPV CHvΔgE-gI_{N69/78/265A}. The steps are based on creating gene restoration strains of gene-deletion viruses using the oligonucleotide primers listed in Table 1.

To rescue the modified virus, plasmids were extracted from the gI mutant infectious clones and then transfected into DEFs cultured in 12-well plates. The transfected cells showed visible fluorescence (EGFP) and cytopathic effect (CPE), and the cell supernatant was collected and stored as viral stock solution. The recombinant viruses were all identified through sequencing. The correctly identified recombinant viruses were designated as DPV CHv-gI_{N69A}, DPV CHv-gI_{N78A}, DPV CHv-gI_{N265A}, DPV CHv-gI_{N69/78/265A}, DPV CHv-gI_{N69/78/265A} repair, and DPV CHvΔgE-gI_{N69/78/265A}.

Viral plaque assay

DEFs on six-well plates were infected with DPV CHv₅₀ or recombinant viruses at a multiplicity of infection (MOI) of 0.0001. After a 2-h adsorption period, the virus solution used to inoculate the cells was removed, and any remaining virus on the cell surface was washed away. The DEFs were then overlaid with MEM containing 1% FBS

Table 1 Primer sequences for overlapping PCR and RT-qPCR

Name	Purpose	Sequence (5′-3′)
pCAGGS-gI-Flag-F	Construct pCAGGS-gI-Flag plasmid	5′-CATCATTTTGGCAAAGAATCGCCACCATGGGAACGACACGACATATACTGATA-3′
pCAGGS-gI-Flag-R		5′-TTGGCAGAGGGAAAAAGATCTTTACTTGTTCATCGTCGCTCTGTAGTCCTTGTTCATCGTCGTCCTTGTAGCTTCTGTGTTTATGATCCCCAGA-3′
pCAGGS-gI _{N69A} -Flag-F	overlapping PCR	5′-CTACCGCCAGTATACGCGGAACTGTCGAGCTA-3′
pCAGGS-gI _{N69A} -Flag-R		5′-CGCGTACTACTGGCGGTAGTTCGGCCTGTGATCC-3′
pCAGGS-gI _{N78A} -Flag-F	overlapping PCR	5′-GAGCTACTAGTATATGCGATTCTCGTCACTGC-3′
pCAGGS-gI _{N78A} -Flag-R		5′-CGCATATACTAGTAGCTCGACAGTTCATTGTA-3′/ 5′-CGCATATACTAGTAGCTCGACAGTTCGCCGTA-3′
pCAGGS-gI _{N265A} -Flag-F	overlapping PCR	5′-ATGCGCCTACGCATGCGGATACCAATAGTGGA-3′
pCAGGS-gI _{N265A} -Flag-R		5′-CGCATGCGTAGGCTGCATATCATCAGATAATGT-3′
pCAGGS-gI _{N69/78/265A} -Kan-F	The Kan fragment was introduced into the recombinant plasmid	5′-GACGACGATGACAAGTAAAGATCTTTCACATCAGTATGACTAAAAGTAAATGTTTTGTTATGATTGACTGTTTTAGGGATAACAGGGTAATCGATTT-3′
pCAGGS-gI _{N69/78/265A} -Kan-R		5′-TTGGCAGAGGGAAAAAGATCTGCCAGTGTTACAACCAAT-3′
gI-repair-F	Amplified complement fragments	5′-CGTACTTCCAGTATTGTCCAGTGCGCCATATAGACGATATATTGAGTTTCAAAAATAGAAATGGGAACGACACGACATATA-3′
gI-Kan-repair-R		5′-TACAAATATATTTGGATGTTAATGAAAGGCAACAGTCAATCATAACAAAACATTTACTTTTGTGCTACTGATGTGAAGCCAGTGTACAACCAAT-3′
UL30-F	RT-qPCR	5′-TTTTCTCTCTCTCGTGAGT-3′
UL30-R		5′-GGCCGGGTTTGCAGAAGT-3′

and 2% methylcellulose (Solarbio, Beijing, China). Five days post-infection, the MEM with methylcellulose was removed, and the cells were fixed with 4% paraformaldehyde (Solarbio, Beijing, China) for 20 min. The cells were then stained with 0.5% crystal violet (Solarbio, Beijing, China) for 5 min. After several washes with PBS, the visible plaques were photographed.

Western blot analysis of recombinant gI

Plasmids pCAGGS-gI-Flag, pCAGGS-gI_{N69A}-Flag, pCAGGS-gI_{N78A}-Flag, pCAGGS-gI_{N265A}-Flag, and pCAGGS-gI_{N69/78/265A}-Flag were transfected into DEFs growing in 12-well plates at a quantity of 1000 ng per well. After 36 h, the cells were lysed using RIPA buffer (Beyotime, China, P0013D). The lysates were centrifuged at 4 °C and 12 000 rpm for ten minutes to obtain a clarified supernatant. The supernatant was mixed with the sample buffer and boiled at 100 °C for 10 min. This mixture was then subjected to 12% sodium dodecyl sulphate–polyacrylamide gel electrophoresis (SDS-PAGE), followed by western blot. For western blot detection, the primary antibodies used were anti-Flag monoclonal antibody (mAb) (M185-3L, MBL) and GAPDH (60 004–1-Ig, Proteintech). The secondary antibody was horseradish peroxidase (HRP)-conjugated goat anti-mouse IgG (SA00001-1, Proteintech). Visualisation was carried out using the Clarity Western ECL system (Bio-Rad, USA).

Deglycosylation of recombinant gI

1000 ng of plasmid DNA per well, including pCAGGS-gI-Flag, pCAGGS-gI_{N69A}-Flag, pCAGGS-gI_{N78A}-Flag, pCAGGS-gI_{N265A}-Flag and pCAGGS-gI_{N69/78/265A}-Flag, was transfected into DEFs cultured in a 12-well plate. At a MOI of 0.01, the recombinant viruses DPV CHV₅₀, DPV CHV-gI_{N69A}, DPV CHV-gI_{N78A}, DPV CHV-gI_{N265A}, and DPV CHV-gI_{N69/78/265A} were used to infect DEFs cultured in 12-well plates individually. After 36 h of transfection or infection, the cells were lysed using RIPA buffer. The lysates were centrifuged at 4 °C, 12 000 rpm for ten minutes to obtain a clarified supernatant. The supernatant was boiled at 100 °C for ten minutes, and Peptide N-glycosidase F (PNGase F) was added following the manufacturer's instructions (P0704S, NEB). The sample was then incubated at 37 °C for one hour for enzymatic deglycosylation. The reactants were subjected to 12% SDS-PAGE and then Western blot analysis. Recombinant virus gI was detected using a mouse polyclonal antibody against DPV gI as the primary antibody, which was prepared in this laboratory. A rabbit polyclonal antibody against DPV VP5 served as a control for viral infection, and GAPDH was used as a loading control.

Subcellular localisation of recombinant gI

For co-localisation analysis, DEFs were plated onto glass slides in 12-well plates. The following transfections or infections were conducted: (1) DEFs were co-transfected with 500 ng of various plasmids pCAGGS-gI-Flag, pCAGGS-gI_{N69A}-Flag, pCAGGS-gI_{N78A}-Flag, pCAGGS-gI_{N265A}-Flag, pCAGGS-gI_{N69/78/265A}-Flag, and 500 ng of pDsRed2-ER. (2) DEFs were co-transfected with 500 ng of pCAGGS-gI-Flag, pCAGGS-gI_{N69/78/265A}-Flag, and 500 ng of pCAGGS. (3) DEFs were co-transfected with 500 ng of pCAGGS-gI_{N69/78/265A}-Flag and 500 ng of pCAGGS-gE-MYC. (4) DEFs were infected with 0.01 MOI of DPV CHV Δ gE-gI_{N69/78/265A} and DPV CHV-gI_{N69/78/265A}. After a 36-h incubation period, an indirect immunofluorescence assay (IFA) following the previously described protocol [32]. The cells were incubated with the specified primary antibody (diluted 1:200) overnight at 4 °C. This was followed by a 2-h incubation with Alexa Fluor 488-conjugated goat anti-mouse IgG (F-2761, Invitrogen) and Alexa Fluor 586-conjugated goat anti-rabbit IgG (T-2769, Invitrogen) as the secondary antibodies (diluted 1:1000). Subsequently, the cells were incubated with 4',6-diamidino-2-phenylindole (DAPI) (D3571, Invitrogen) at room temperature for 5 min. Finally, the glass slides were examined under a fluorescence microscope.

Co-immunoprecipitation

1000 ng of pCAGGS-gI-Flag, pCAGGS-gI_{N69A}-Flag, pCAGGS-gI_{N78A}-Flag, pCAGGS-gI_{N265A}-Flag and pCAGGS-gI_{N69/78/265A}-Flag along with 1000 ng of pCAGGS-gE-MYC were transfected into HEK 293 T cells. Following transfection for 36 h, the cells were lysed using RIPA buffer. The lysate was centrifuged at 4 °C, 12 000 rpm for ten minutes to obtain a clarified supernatant. Following the centrifugation, 0.5 mL of the cell lysate from each sample was taken and incubated with 10 μ g of the specified antibody and 1 mg of SureBeads Protein G (Thermo Fisher Scientific, Waltham, MA, USA) at room temperature for 2 h. The SureBeads Protein G were washed three times with PBST (phosphate buffer solution with Tween) and centrifuged at 13 000 \times g for 1 min. Finally, the precipitates were resolved by 12% SDS-PAGE, and a western blot was performed using appropriate antibodies. The blots were visualised using the Clarity Western ECL system.

In vivo experiments

At 14 days of age, ducks were inoculated with 10⁶ TCID₅₀ DPV CHV₅₀ ($n=10$), DPV CHV-gI_{N69/78/265A} ($n=10$), DPV CHV-gI_{N69/78/265A} repair ($n=10$), and MEM ($n=10$), respectively. The ducks in each group were continuously monitored for clinical signs, including percentage

survival, rectal temperature, and body weight. Afterwards, 14-day-old ducks were re-inoculated with 10^6 TCID₅₀ DPV CHV₅₀ ($n=10$), DPV CHV-gI_{N69/78/265A} ($n=10$), DPV CHV-gI_{N69/78/265A} repair ($n=10$), and MEM ($n=10$), respectively. Infected ducks were regularly autopsied, internal organs were collected, and micro-pathological sections were made to observe the histopathological changes of different organs. At the end of the experiment, all surviving ducks were humanely euthanised.

Quantification of DPV gene copy number

The genome copy number of DPV in duck viscera was measured to determine the viral load. Samples of heart, liver, spleen, glandular stomach, duodenum, cecum, bursa of Fabricius, and thymus were collected from infected animals at 2, 5, 8 and 10 days after infection. Virus replication in vivo was monitored by quantifying the DPV gene copy number. DNA was extracted from all samples using a cell and tissue genomic DNA extraction kit following the manufacturer's instructions (Magen; Catalog number: D3191-03). The DPV genome copy number was detected by qPCR [32].

Data analysis

All experiments were conducted three times, and statistical analysis was performed using GraphPad Prism 9. Virus plaque size data was analysed using one-way analysis of variance (ANOVA). The survival curve of ducks was analysed using the logarithmic rank (Mantel-Cox) test. The viral load of recombinant virus in different tissues was analysed using a *t*-test. The *P* value of less than 0.05 was considered statistically significant.

Ethics statement

All one-day-old ducks were purchased from a farm operated by Sichuan Agricultural University (Sichuan, China). The ducks were free of DPV and tested negative for DPV antibodies. They were housed in the animal facilities at Sichuan Agricultural University in Chengdu, China. This study was approved by the Experimental Operation Guidelines and Animal Welfare Committee of Sichuan Agricultural University (Approval license No. XF2014-18).

Results

Conservative analysis of gI N-glycosylation sites in *Alphaherpesvirinae*

The detailed alignment of multiple sequences of gI showed differences between species in predicting N-glycosylation sites in the *Alphaherpesvirinae*. Protein N-glycosylation is a post-translational modification that usually happens on the N-X-(S/T) consensus sequence,

where X is any amino acid except proline. However, not all N-X-(S/T) sequences are glycosylated, indicating that while the N-X-(S/T) motif is necessary for protein glycosylation, it is insufficient. A comparative analysis of the primary structures of gI from six *Alphaherpesvirinae* species, as shown in Figure 1, reveals that all species have three or more predicted N-glycosylation sites, but these sites are not conserved. DPV gI is a type I transmembrane glycoprotein consisting of an extracellular domain (ETD), a transmembrane domain (TMD), and a cytoplasmic domain (CTD). Its ETD is rich in asparagine residues and contains three potential N-glycosylation consensus sequences. This analysis emphasises the complexity and variability of N-glycosylation in *Alphaherpesvirinae* and stresses the need for a deeper understanding of the role of glycosylation in viral pathogenesis.

Generation of recombinant viruses with mutations at each potential N-glycosylation site on the DPV gI through the DPV genetic operating system

DPV gI has potential N-glycosylation sites at the following locations: Asn₆₉, Asn₇₈, and Asn₂₆₅. We created recombinant viruses to study how gI N-glycosylation affects recombinant viruses and their impact on ducks, as shown in Figure 2A. Using the DPV genetic operating system, we employed a two-step recombination mediated by Red. This process involves the first recombination for inserting PCR amplification of the selective marker and a second recombination for removing the Kan insertion marker using the *I-SceI* cutting step. The system has been widely used for marker-free modification of large DNA molecules, such as the duck plague virus genome cloned into *Escherichia coli* bacterial artificial chromosome (BAC).

In Figure 2B, all viruses displayed green fluorescence (EGFP) following transfection. The gI gene of the recombinant virus underwent sequencing, and comparison with the DPV CHV strain genome confirmed the absence of additional mutations in the F1 generation. These findings suggest that all recombinant viruses, including DPV CHV-gI_{N69A}, DPV CHV-gI_{N78A}, DPV CHV-gI_{N265A}, DPV CHV-gI_{N69/78/265A}, DPV CHV-gI_{N69/78/265A} repair, and DPV CHV Δ gE-gI_{N69/78/265A}, were successfully rescued.

The effects of mutations at each potential gI N-glycosylation site on the electrophoretic mobility in both the presence and absence of PNGase F

To compare the molecular weight (MW) differences of each recombinant gI, we analysed cell lysates from the transfected cells using Western blot. Due to the addition of multiple Flag tags, the MW of the detected gI-Flag is about 70 kDa, which is higher than predicted (Figure 3A, Lane 1). However, all modified gI proteins

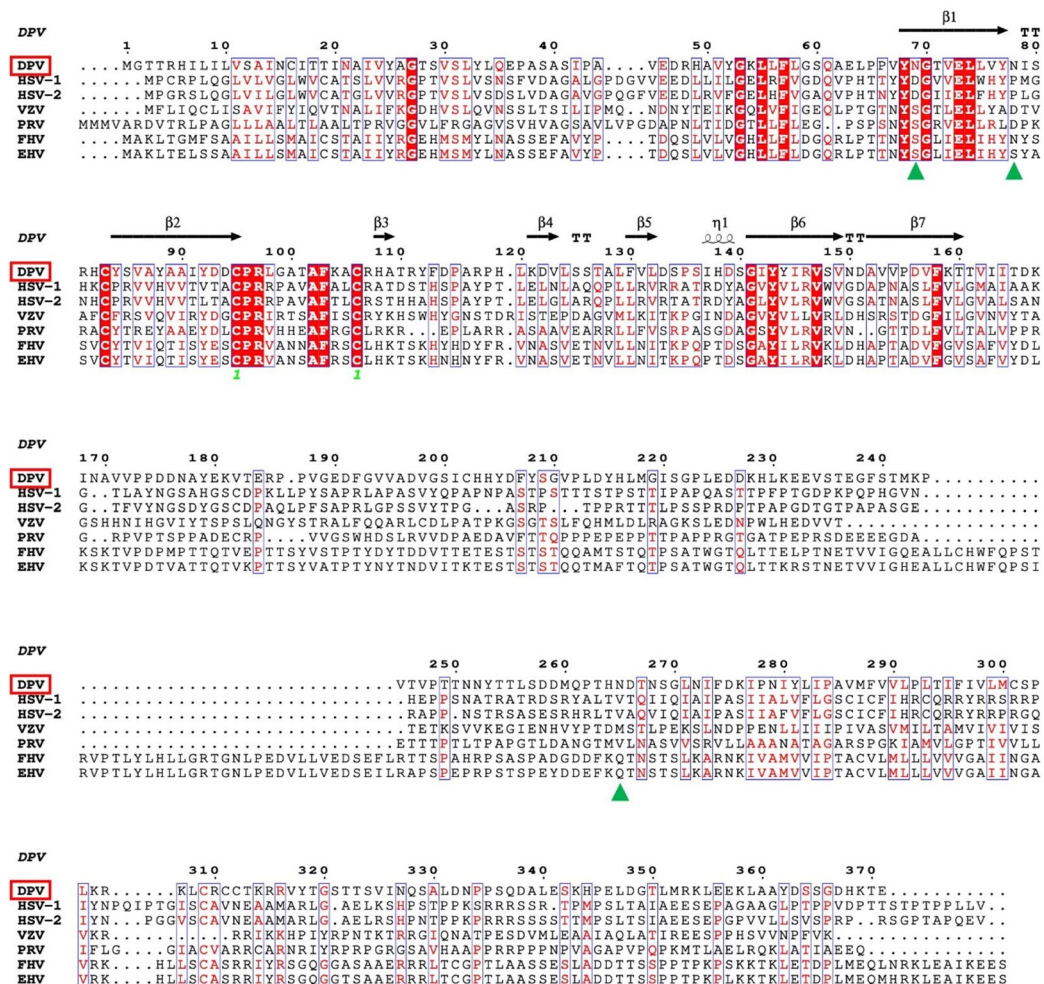


Figure 1 Based on the secondary structure of DPV gI, the sequence alignment of the Alphaherpesvirus gI sequence was conducted.

Overall, conserved residues are represented with a red background, highly conserved residues are indicated by red characters, and regions with a high degree of conservation are framed in blue. The secondary structure of DPV gI is displayed above the alignment, with α -helices represented as small wavy lines, beta-strands depicted as arrows, and strict β -turns denoted by the letter "T" in a TT configuration. Conserved disulfide bonds are indicated below the sequence with green numerals. Green triangles denote potential N-glycosylation sites. The accession numbers for the *Alphaherpesvirus* gI sequences are as follows: Herpes simplex virus type 1 (HSV-1), AAW49017.1; Herpes simplex virus type 2 (HSV-2), AWP48734.1; Varicella-zoster virus (VZV), AAK01046.1; Pseudorabies virus (PRV), UQK92472.1; Feline herpesvirus (FHV), WMD92286.1; Equine herpesvirus (EHV), YP_010795113.1.

show lower MW and the gI_{N69/78/265A}-Flag migrates more quickly than individual mutants, including gI_{N69A}-Flag, gI_{N78A}-Flag, and gI_{N265A}-Flag (Figure 3A, Lanes 2, 3, 4 and 5).

Cell lysate was collected, treated with or without PNGase F, and analysed by western blot. The results in Figure 3B show that all gI mutants migrate faster than gI in denaturing gels. After treating the infected cell lysates with PNGase F, all gI mutants exhibited a migration rate in denaturing gels that was as slow as gI. We observed the same pattern in the natural viral infection and the over-expression form through plasmid transfection. The levels of all gI mutants detected by Western blot were similar to

those of wild-type gI. These results suggest that gI is glycosylated at each of the three potential N-glycosylation sites without affecting the virus accumulation in infected cells.

Deglycosylation affects the subcellular localisation of recombinant gI

During biosynthesis, membrane proteins initially receive a mannose-rich core polysaccharide precursor in the endoplasmic reticulum and then develop into heterozygous or complex oligosaccharides in the Golgi apparatus. We wanted to find out if gI mutants gather in the cellular compartments of the secretory

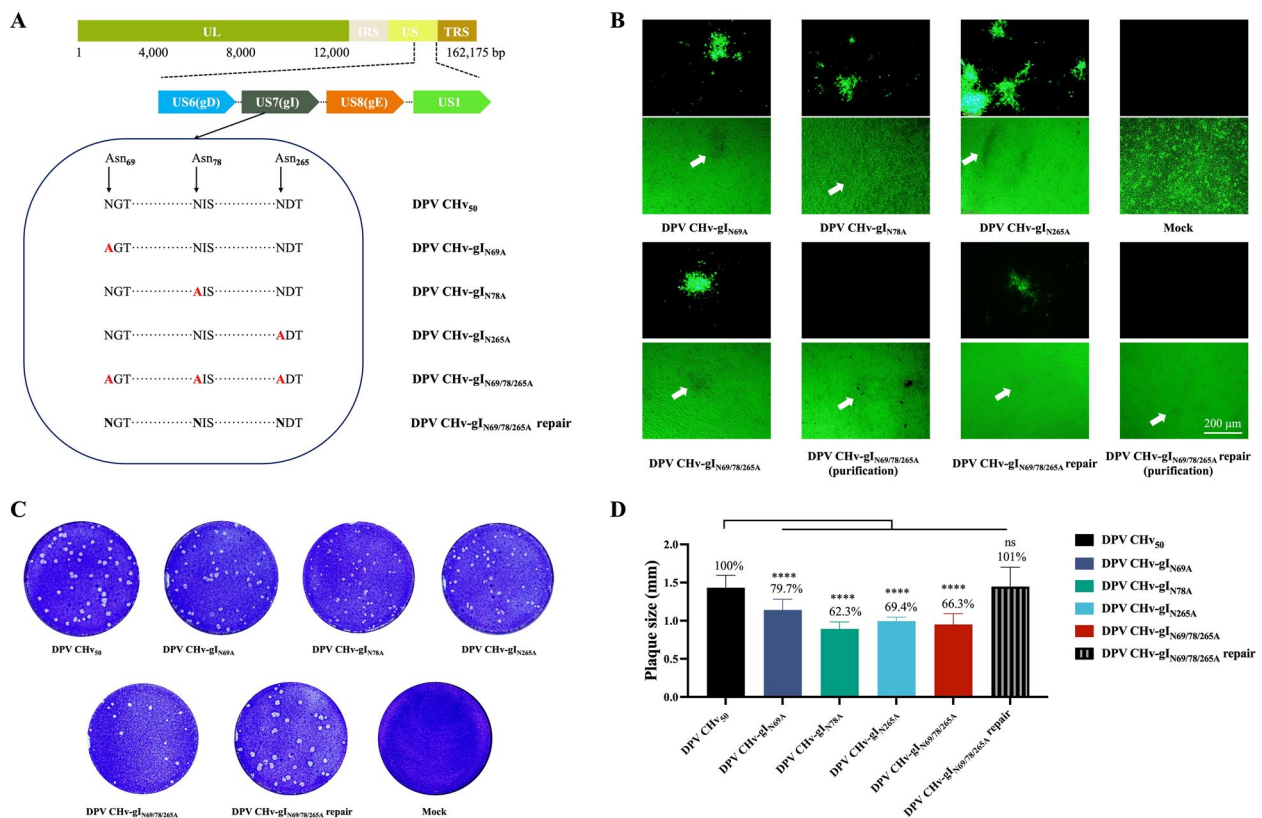


Figure 2 Recombinant virus rescue and extracellular characterisation of the gI N-glycosylation site mutation in the DPV CHv strain. **A** Schematic representation of the gI N-glycosylation site mutation in the DPV CHv strain. **B** Following the transfection of plasmids containing the plasmid infectious clones (pDPV CHv-gI_{N69A}, pDPV CHv-gI_{N78A}, pDPV CHv-gI_{N265A}, pDPV CHv-gI_{N69/78/265A}, pDPV CHv-gI_{N69/78/265A} repair, and pDPV CHvΔgE-gI_{N69/78/265A}), the successful rescue of the virus was indicated by the observation of EGFP under a fluorescence microscope, while CPE was monitored using a light microscope. Cells transfected with the mock plasmid served as the control group. **C** Crystal violet staining was utilised to assess viral plaques. **D** Fifteen plaques were randomly selected per group for measurement of plaque diameter using Image J software (ns indicates not significant, $P > 0.05$; *, $P < 0.05$; **, $P < 0.01$; ***, $P < 0.001$; ****, $P < 0.0001$; t-test).

pathway. To investigate this, we co-labelled DEFs with Flag antibody and an ER-specific fluorescent marker. The Flag antibody can mark both gI and its mutant forms. The results showed that gI single N-glycosylation site mutant did not co-locate with ER in DEFs, but gI_{N69/78/265A}-Flag co-located with ER in DEFs when all of its N-glycosylation sites were mutated. Does mutation of all N-glycosylation residues reduce the surface levels of gI in DEFs? Our observations showed that the localisation of gI_{N69/78/265A}-Flag and the Golgi marker protein GM130 in DEFs was severely impaired. However, we found that gI_{N69/78/265A}-Flag could co-localise with GM130 only in the presence of gI's complex partner gE (Figure 4). In conclusion, our data on the subcellular localisation confirmed that the subcellular positioning of recombinant gI was affected only after all N-glycosylation sites were mutated. The mutated gI is mistakenly retained within the internal secretory compartments, causing transport defects. However, its

interacting protein, gE, can carry deglycosylated gI to the Golgi compartment.

gI/gE complex formation is not affected by the mutation of the gI N-glycosylation site

N-glycosylation is crucial in various cellular protein structure and function processes, including protein-protein interactions. In herpesvirus, gI typically forms a complex with gE, which is involved in virus intercellular transmission and assembly. To investigate the impact of mutations at the gI N-glycosylation site on the subcellular localisation of recombinant gI, we observed that gI_{N69/78/265A}-Flag could only co-locate with GM130 in DEFs in the presence of gE. This led us to speculate that the gI N-glycosylation site mutation would not disrupt the formation of the gI/gE complex. To verify this speculation, we conducted immunoprecipitation experiments, which showed that mutations at the gI N-glycosylation site, whether single or total, did not affect

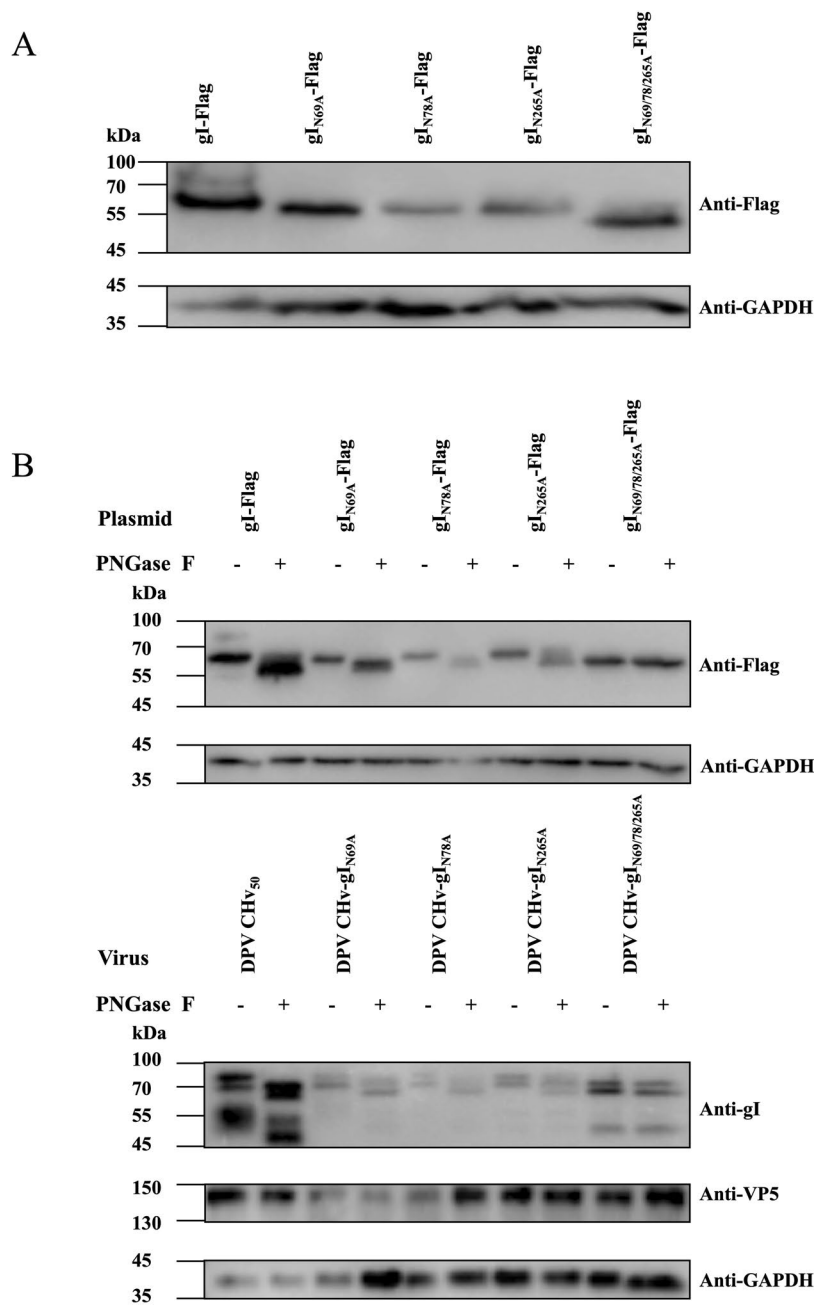


Figure 3 Recombined gI MW and deglycosylation analysis. (A) DEFs were transfected with gI expression plasmids (pCAGGS-gI-Flag, pCAGGS-gI_{N69A}-Flag, pCAGGS-gI_{N78A}-Flag, pCAGGS-gI_{N265A}-Flag, and pCAGGS-gI_{N69/78/265A}-Flag) at a dose of 1000 ng per well. Western blot analysis was performed on cell lysates 36 h post-transfection, and recombinant gI proteins were detected using a mouse monoclonal anti-Flag antibody: gI-Flag (lane 1), gI_{N69A}-Flag (lane 2), gI_{N78A}-Flag (lane 3), gI_{N265A}-Flag (lane 4), and gI_{N69/78/265A}-Flag (lane 5). (B) Collect the cell lysates from DEFs transfected with recombinant gI plasmids, and treat them with PNGase F at 37 °C for 1 h. The digested products of PNGase F are then subjected to 12% SDS-PAGE, followed by western blot. Recombinant gI is analysed using a mouse monoclonal anti-Flag antibody, with GAPDH serving as a loading control. Similarly, cell lysates from DEFs infected with recombinant viruses were processed in the same manner. Analysis of recombinant gI using a mouse polyclonal anti-gI antibody, with a rabbit polyclonal anti-VP5 antibody serving as a control for viral infection, and GAPDH as a loading control. The results presented are representative of three independent experiments.

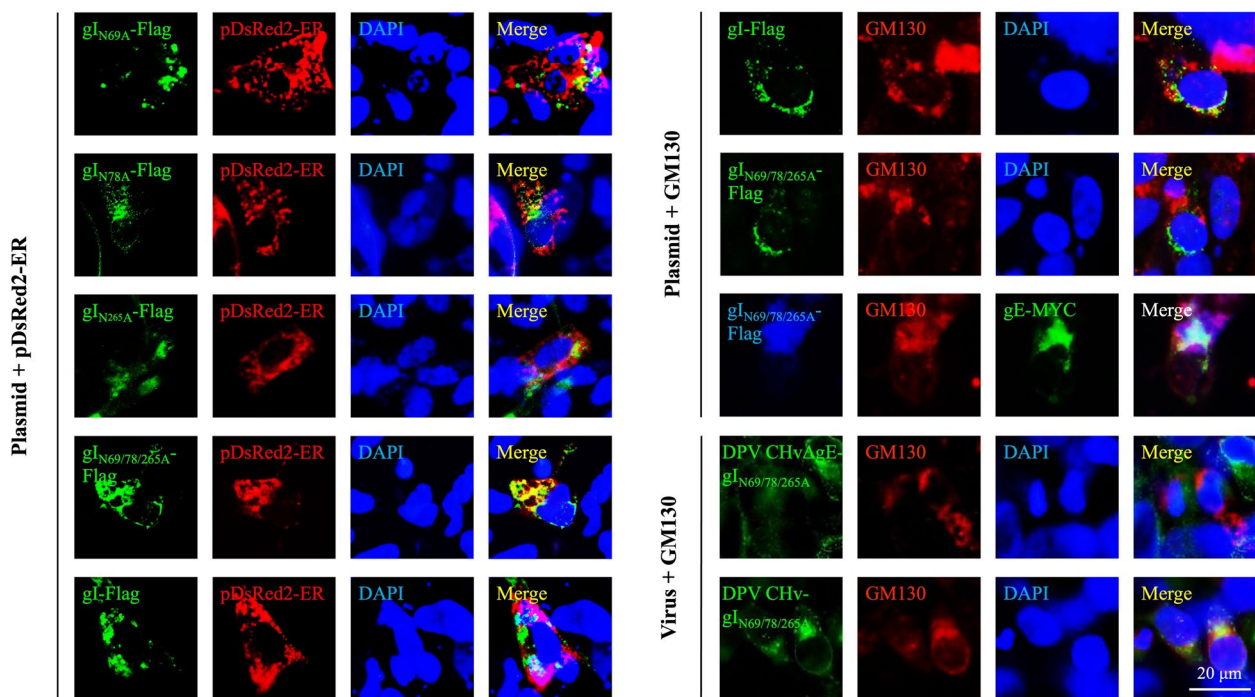


Figure 4 Subcellular localisation of recombinant gI protein. (1) The recombinant gI plasmids (pCAGGS-gI-Flag, pCAGGS-gI_{N69A}-Flag, pCAGGS-gI_{N78A}-Flag, pCAGGS-gI_{N265A}-Flag, and pCAGGS-gI_{N69/78/265A}-Flag) were co-transfected with pDsRed2-ER into DEFs. (2) The pCAGGS-gI-Flag and pCAGGS-gI_{N69/78/265A}-Flag plasmids were individually transfected into DEFs, while the pCAGGS-gI_{N69/78/265A}-Flag and pCAGGS-gE-MYC plasmids were co-transfected into DEFs, and their localisation was marked using GM130. (3) DPV CHvΔgE-gI_{N69/78/265A} and DPV CHv-gI_{N69/78/265A} were respectively used to infect DEFs, and their localisation was similarly marked using GM130. Transfection or infection was carried out, and IFA was performed after 36 h. Fluorescence microscopy was used for visualisation (magnification: 600×; scale bar: 20 μm).

the formation of gI/gE complex (Figure 5). IFA experiments also yielded the same result (data not shown).

Exogenous growth kinetics of gI N-glycosylation site mutants

In our study, we investigated the size of viral plaques. We found that the diameter of plaques formed by cells infected with gI N-glycosylation site mutants was significantly smaller than that of cells infected with DPV CHv₅₀. We randomly selected 15 plaques from each group, measured their diameter using ImageJ software, and then performed statistical analysis using GraphPad Prism 9 software. Our results, shown in Figures 2C, D, indicated that the plaque diameter formed by DPV CHv-gI_{N69/78/265A} was about 66.3% of that of DPV CHv₅₀. We also observed that point mutants of gI N-glycosylation affected the plaque diameter of infected cells. Based on these findings, we tentatively concluded that gI N-glycosylation is involved in the late stage of DPV replication.

gI N-glycosylation promotes the pathogenesis and lethality of duck plague

To investigate whether gI N-glycosylated mutants play a role in the pathogenesis of DPV, we infected 14-day-old

ducks with the virus at a concentration of TCID₅₀, as shown in Figure 6A. We then observed the infected ducks for ten consecutive days. In the DPV CHv-gI_{N69/78/265A} group, only two ducks had rectal temperatures exceeding 42.5 °C on the third day post-challenge. The rest of the ducks maintained body temperatures, albeit fluctuating, within the normal range throughout the monitoring period, and their body weight increased steadily at an average daily gain of 3.61 g per duck. No mortality was recorded in this group. In the control group (MEM), all ducks maintained body temperatures within the normal range, consistently increasing body weight at an average daily gain of 3.86 g per duck, and no mortality occurred. In the DPV CHv₅₀ group, nearly all ducks had rectal temperatures exceeding 42.5 °C post-inoculation from day one to five. Some ducks' temperatures even rose above 43.5 °C. Between the second and sixth days, there was no significant increase in body weight. However, after the sixth day, body weight continuously increased. Mortality was first observed on the fifth-day post-inoculation, with the peak of mortality occurring on the sixth day, during which two ducks died. Four ducks died during the monitoring period, resulting in a mortality rate of 40%.

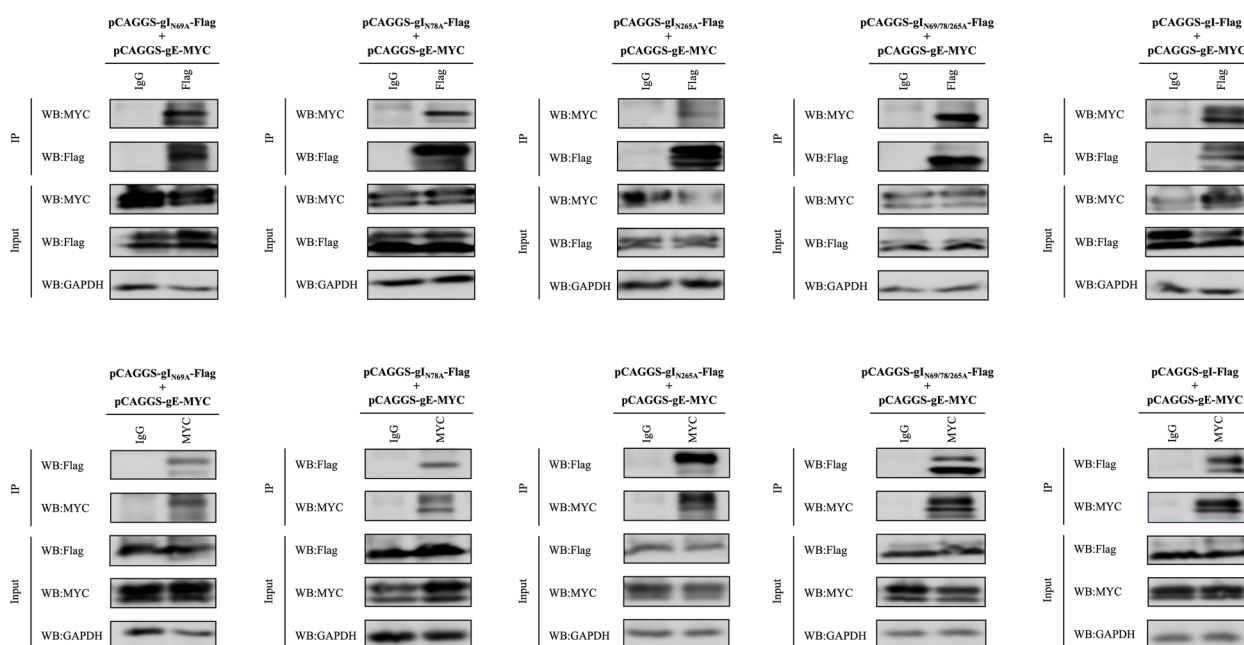


Figure 5 CO-IP was utilised to examine the interaction between gI and gE after the deglycosylation of gI. The recombinant gI plasmids (pCAGGS-gI-Flag, pCAGGS-gI_{N69A}-Flag, pCAGGS-gI_{N78A}-Flag, pCAGGS-gI_{N265A}-Flag, and pCAGGS-gI_{N69/78/265A}-Flag) with the pCAGGS-gE-MYC plasmid and cotransfect them into HEK 293 T cells for 36 h. For the immunoprecipitation (IP) process, the Anti-Flag antibody was utilised for the direct capture of interacting proteins, while the Anti-MYC antibody was employed for the reverse capture of interacting proteins. IgG antibody was used as a mock control to ensure specificity. For immunoblotting (IB), anti-Flag and anti-MYC antibodies were applied to detect the presence of the targeted proteins. The results presented are representative of three independent experiments.

To eliminate the effects of non-target mutations, we used DPV CHV-gI_{N69/78/265A} repair to infect ducks. The rectal temperature exceeded 42.5 °C from days two to five, and the body weight hardly increased during this period. However, it continued to increase after day five. Mortality was observed on the 5th day post-infection, with a total of five deaths recorded during the monitoring period, resulting in a mortality rate of 50% (Figures 6B–D). The data indicated that gI N-glycosylation mutants could somewhat reduce the virus virulence.

gI N-glycosylation mutation inhibits DPV-induced pantropic tissue damage and its replication in vivo

Next, to address whether gI N-glycosylation mutations inhibit DPV replication in vivo, we monitored tissue lesions and viral loads in infected animals throughout the experiment. Death occurred in the DPV CHV₅₀ and DPV CHV-gI_{N69/78/265A} repair-infected ducks. Postmortem observations showed that the dead ducks showed systemic sepsis symptoms, including bleeding spots on the heart surface, severe liver congestion and necrosis, spleen enlargement, bleeding and soft texture, glandular stomach, duodenum, cecum, bursa of Fabricius and thymus haemorrhage and atrophy. However, there were no deaths in the DPV CHV-gI_{N69/78/265A} group. Anatomical observation of surviving ducks showed spleen

haemorrhage and enlargement, slight haemorrhage of the thymus, and no obvious lesions in other organs (Figure 7A). The histopathological section results showed that in the DPV CHV-gI_{N69/78/265A} group, infected ducks' tissues such as the heart, liver, spleen, glandular stomach, duodenum, cecum, and bursa of Fabricius did not exhibit significant lesions compared to the MEM group, with minor reticular necrotic areas observed in the thymus tissue. In contrast, ducks infected with DPV CHV₅₀ and the DPV CHV-gI_{N69/78/265A} repair group exhibited myocardial fibre rupture in the heart; congestion in the hepatic tissue vessels and sinusoids, with severe fatty degeneration of the liver tissue; areas of necrosis in the spleen devoid of cellular components, presenting a reticular pattern; necrosis of the deep tubular glands in the glandular stomach; mucosal epithelial shedding and villous breakage in the duodenum and cecum; indistinct corticomedullary boundaries in the bursa of Fabricius; and thymic lymphocyte necrosis and fragmentation, filled with a large amount of pale red interstitial tissue and red blood cells (Figure 7B). During the monitoring process, it was observed that the head and neck of ducks in the DPV CHV₅₀ and DPV CHV-gI_{N69/78/265A} repair infected group were enlarged, and the eyelids were soaked, showing typical symptoms of "Big Head Plague" (Figure 7C). The ducks in the DPV CHV-gI_{N69/78/265A}-infected group

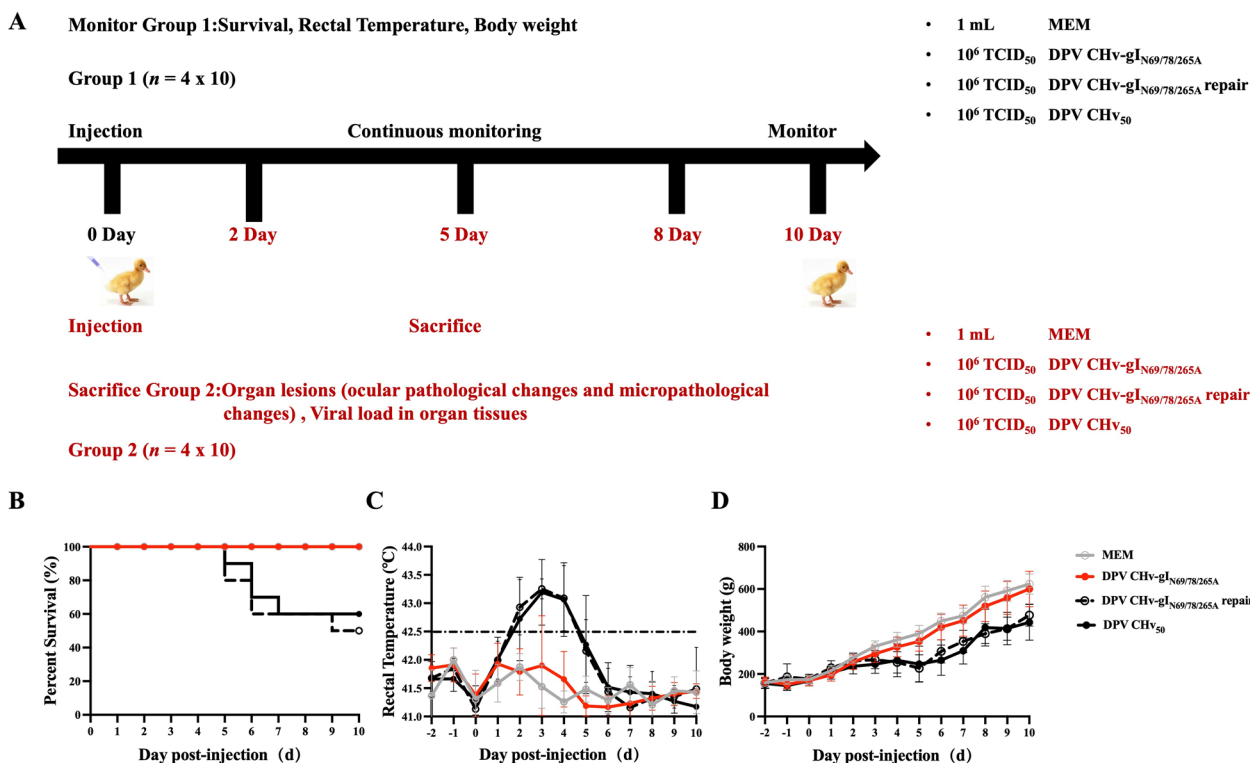


Figure 6 In vivo experiments. **A** Schematic representation of the experimental procedure investigating the impact of gI N-glycosylation on DPV. At 14 days old, ducks were intramuscularly injected with DPV CHv₅₀, DPV CHv-gI_{N69/78/265A}, DPV CHv-gI_{N69/78/265A} repair, and MEM (10⁶ TCID₅₀). Ducks injected with MEM served as negative controls. Group 1 (n=40, 10 ducks per group) was used to determine the survival rate, rectal temperature, and body weight of the ducks. Group 2 (n=40, 10 ducks per group) was euthanised at 2, 5, 8, and 10 days post-inoculation to assess pathological changes in different organs and viral load. **B–D** Survival curves (**B**), rectal temperature (**C**), and body weight (**D**) of ducks inoculated with the specified viruses. The data were analysed using the Mantel-Cox log-rank test.

showed no obvious changes in the appearance of the head as in the MEM group. Interestingly, in the later stages of viral infection, the thymus of ducks in the DPV CHv₅₀ group shrank to only 13.4% to 35.4% of those in the MEM group (Figure 7D). These results suggest that gI N-glycosylation is involved in the pathogenesis of DPV, which partially prevents DPV-induced thymus atrophy.

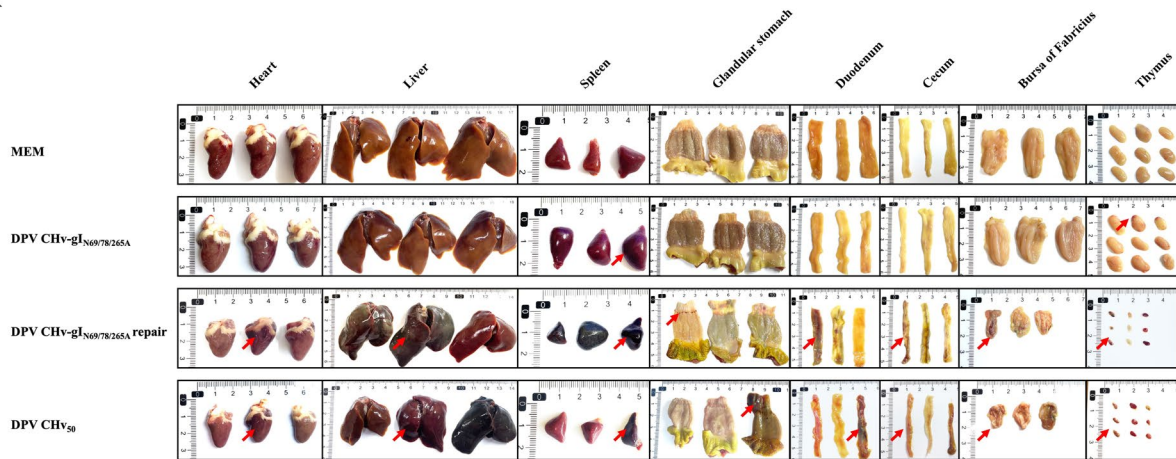
The virus replication in different tissues and organs of infected ducks was measured using qPCR at various time points. On the fifth day post-infection, the range of viral copy numbers in multiple organs of the DPV CHv-gI_{N69/78/265A} group ducks was from 10^{5.62} to 10^{7.39} copies/0.1 g, with the highest viral content found in the thymus. The viral content in various organs of ducks in the DPV CHv₅₀ and DPV CHv-gI_{N69/78/265A} repair groups was generally higher than that in the DPV CHv-gI_{N69/78/265A} group. The range of viral copy numbers in the organs of ducks in the DPV CHv₅₀ group was from 10^{7.94} to 10^{10.17} copies/0.1 g, while the range of viral copy numbers in the organs of ducks in the DPV CHv-gI_{N69/78/265A} repair group was from 10^{7.78} to 10^{10.11} copies/0.1 g. At this point, the average viral copy number in

the DPV CHv-gI_{N69/78/265A} group was 100.1 times lower than that in the DPV CHv₅₀ group and 92.5 times lower than that in the DPV CHv-gI_{N69/78/265A} repair group.

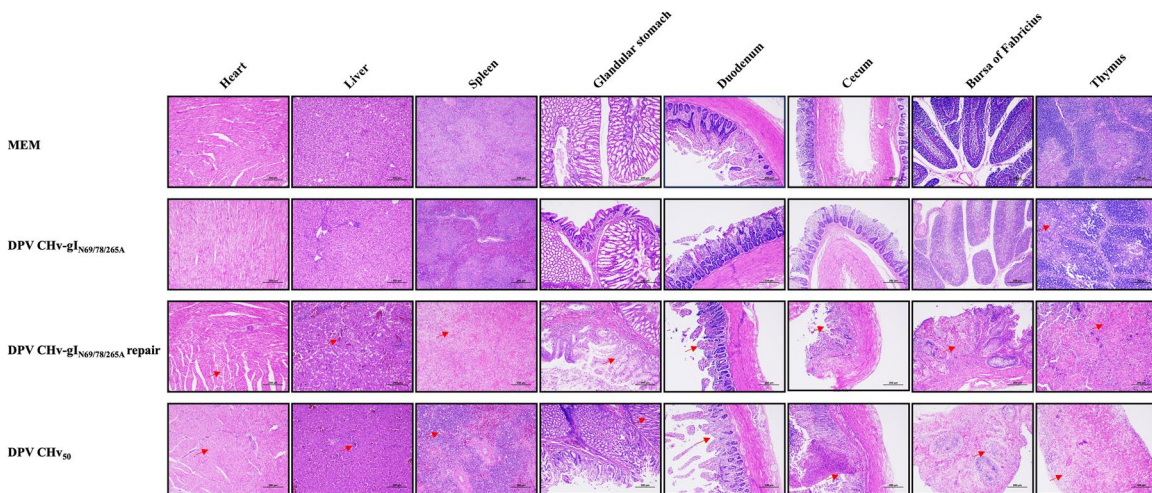
On the tenth day post-infection, there was a significant decrease in viral copy numbers in the organs of ducks across all groups. The range of viral copy numbers in the organs of the DPV CHv-gI_{N69/78/265A} group was from 10^{4.3} to 10^{6.04} copies/0.1 g. In the DPV CHv₅₀ group, the organ's viral copy numbers in the organs ranged from 10^{5.5} to 10^{6.58} copies/0.1 g. In the DPV CHv-gI_{N69/78/265A} repair group, the organ's viral copy numbers ranged from 10^{5.46} to 10^{6.42} copies/0.1 g. At this time, the average viral copy number in the DPV CHv-gI_{N69/78/265A} group was 3.2 times lower than that in the DPV CHv₅₀ group and 2.5 times lower than that in the DPV CHv-gI_{N69/78/265A} repair group (Figures 8A–H).

Since antibodies have been produced in the ducks, each group of surviving ducks at this time has some resistance to death. In general, the replication level of DPV in ducks after gI N-glycosylation mutation was lower than that in the DPV CHv₅₀ and DPV CHv-gI_{N69/78/265A} repair group. The decrease in viral replication ability was one of

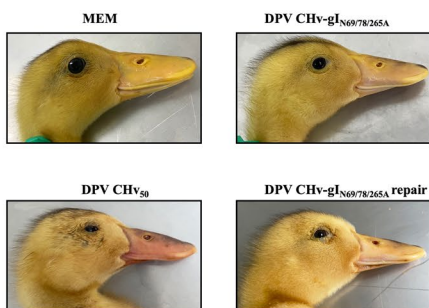
A



B



C



D

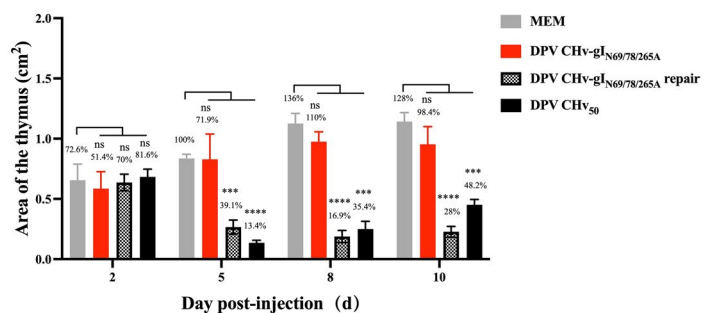


Figure 7 Autopsy histopathology of designated viruses-infected ducks. **A** At day 5 post-infection with the designated viruses (DPV CHV₅₀, DPV CHV-gI_{N69/78/265A}, DPV CHV-gI_{N69/78/265A} repair, and MEM), ducks were subjected to necropsy, and histopathological lesions in various tissues were documented. **B** Histological analysis of the heart, liver, spleen, glandular stomach, duodenum, cecum, bursa of Fabricius and thymus after infection with designated viruses. (haematoxylin and eosin staining, 100× magnification). **C** Records of the characteristic features of ducks' heads during the disease phase following infection with the designated viruses. **(D)** Infection with DPV CHV₅₀ leads to atrophy of the thymus. Each group's thymus area of ducks was scanned and measured using ImageJ. The results were calculated based on the thymus area of the control group ducks on the 5th day as 100% (ns, $P > 0.05$; *, $P < 0.05$; **, $P < 0.01$; ***, $P < 0.001$; ****, $P < 0.0001$; t-test).

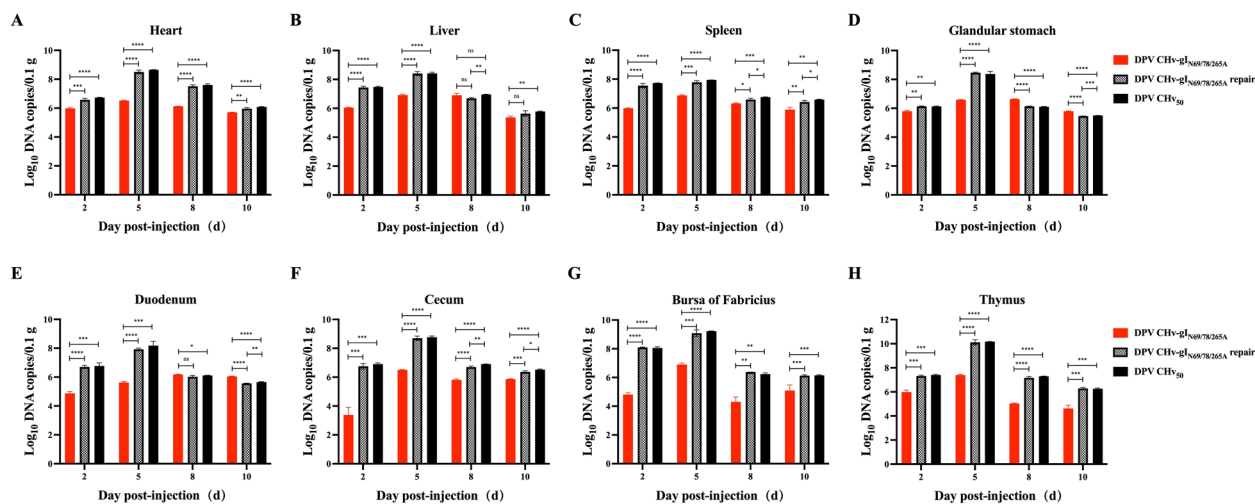


Figure 8 Replication characteristics of gI N-glycosylation mutant recombinant virus in ducks. **A–H** Quantitative determination of the designated virus DPV genomic copy number in the heart (**A**), liver (**B**), spleen (**C**), glandular stomach (**D**), duodenum (**E**), caecum (**F**), bursa of Fabricius (**G**), and thymus (**H**) of experimentally infected ducks (ns, $P > 0.05$; *, $P < 0.05$; **, $P < 0.01$; ***, $P < 0.001$; ****, $P < 0.0001$; t -test) 5'.

the reasons for the absence of disease and death in ducks. Therefore, N-glycosylation of gI plays a role in the function of gI as a virulence factor.

Discussion

Glycoprotein I (gI) is encoded by the US7 gene and plays various roles in viral infection. It has been reported that gI forms a heterodimeric complex with glycoprotein E (gE) on the cell membrane, modulating the translocation of progeny viruses to intercellular junctions and directly participating in cell-to-cell spread [33, 34]. gI utilizes endoplasmic reticulum (ER)-associated degradation components Derlin-1 and Sec61 to facilitate the ubiquitination of Toll-like receptors 3 (TLR3) and 4 (TLR4), thereby assisting the virus in evading host immune surveillance [35]. The interaction between gI and gamma-secretase modulates the excessive phosphorylation of tau protein and beta-amyloid ($A\beta$), thereby elevating the risk of neurodegenerative disorders [36]. Additionally, gI acts as a virulence gene, reducing the virulence of the virus to the host when deleted in many herpes viruses [37–39]. However, the function of gI as a glycoprotein in viral infection remains unclear.

Glycoproteins can capture N-linked and O-linked glycans. Previous studies have shown that by using an O-Glycosidase & Neuraminidase Bundle, β 1-4 Galactosidase-S, and β -N-Acetylglucosaminidase S to cleave O-glycosidic sugar chains, and PNGaseF to cleave N-glycosidic sugar chains, the occurrence of O-glycosylation and N-glycosylation of DPV gI can be determined based on the changes in protein size. At the plasmid level, the MW of gI only changes upon

cleavage with PNGaseF. Thus, we focused on exploring the role of N-glycosylation of gI in virulence during viral infection. We generated recombinant DPV viruses with N-glycosylated mutations using a reverse genetic system and demonstrated that N-glycosylation of DPV gI affects viral replication and pathogenesis in vivo.

When comparing the gI gene sequences of Alphaherpesviruses, we found that the expected N-glycosylation sites in the DPV gI were not conserved. However, in our secondary structure model, N₆₉ and N₇₈ are positioned at the ends of the protein surface β -strand regions. At the same time, N₂₆₅ is buried near the lipid membrane, all within conserved structural folds. The N₆₂₀ residue of VZV gB corresponds to the N₆₃₆ residue of PRV. Both are located within the conserved DIV β -strand and are part of the epitope recognised by neutralising antibody (93 k) against VZV gB [40, 41]. KSHV gH ELEFN₅₀₋₅₄ is also a potential glycosylation site within the presumed β -hairpin of the KSHV gH/gL interaction region. When ELEFN₅₀₋₅₄ is mutated to ELAAN, glycosylation is reduced, leading to decreased binding with EphA2 and a subsequent reduction in fusion [42]. N-glycosylation sites within SAV glycoprotein are not highly conserved. E₁₃₅N is located on the surface area within the predicted central β -strand, while E₂₃₁₉N is embedded near the lipid membrane [43]. Many flaviviruses possess highly conserved N-glycosylation sites at positions Asn₁₃₀ and Asn₂₀₇, which play a role in mouse viral replication and neurovirulence. These sites are also situated at the terminal regions of the β -strand [44]. This strongly supports DPV gI N₆₉, N₇₈, and N₂₆₅ as functional N-glycosylation sites.

N-glycosylation is a common post-translational modification that is essential for the localization and secretion of proteins, enabling them to perform their functions at the appropriate location. This is particularly crucial for virulence genes [45], as abnormal glycosylation can result in the loss of pathogenicity in infectious agents [46]. In general, removing the sugar molecules or altering the glycosylation sites due to the use of glucosidase inhibitors may cause the viral glycoproteins to fold incorrectly and be retained in the ER [47, 48]. Therefore, it is important to investigate how mutations at the glycosylation sites could impact the subcellular localisation of gI. The findings showed that mutating a single N-glycosylation site in gI did not affect its subcellular localisation. However, when the three N-glycosylation sites of gI are mutated at the same time, the gI is trapped in the ER. When present with gE, gE can interact with the deglycosylated gI and carry it to the Golgi apparatus. The analysis of viral glycoprotein glycosylation typically focuses on studying recombinant proteins. These proteins are usually produced in cell lines with different glycosylation capabilities compared to the host cells. As a result, the glycosylation patterns of the resulting recombinant glycoproteins may differ from those of the native viral proteins [49]. We then looked into localisation of all N-glycosylation mutations of gI at the viral level, and the results are shown in Figure 4. The localisation patterns of the native viral proteins matched those of the recombinant proteins expressed from heterologous plasmids. We believe that structural changes caused by deglycosylation of gI might affect other processes within the viral life cycle, such as the assembly of viral particles, which could be detrimental for viral infection and proliferation (Figures 2C and 2D). However, the conformational changes do not hide the binding site for gE, and therefore, do not affect its ability to bind with gE (Figure 5).

It is undisputed that using animal samples to analyse the mechanisms of infection of animal pathogenic viruses is crucial for understanding their pathogenic mechanisms in animals. The gap between observations of viral infection *in vitro* and *in vivo* is significant. Therefore, evaluating *in vivo* samples should provide more valuable information on the mechanisms of infection than evaluating *in vitro* samples.

In this study, we also measured viral loads of infected ducks in different tissues: heart, liver, spleen, glandular stomach, duodenum, cecum, bursa of Fabricius, and thymus. Unlike replication on DEFs *in vitro* DPV CHV-gI_{N69/78/265A} (data not shown), the virus proliferation in ducks was significantly reduced. When detecting the lesions of various parenchymal organs related to the

characteristics of duck plague, one of the characteristics of duck plague is the degeneration of systemic parenchymal organs [50].

Compared with DPV CHV₅₀, DPV CHV-gI_{N69/78/265A} resulted in significantly lower virus copy numbers in different tissues. The most significant difference was on day five after injection. At that time, the DPV CHV₅₀ infected group was near the death peak, and the ducks' antibodies could not resist the virus replication in the body. Meanwhile, as shown in Figure 7A, the bleeding of the bursa of Fabricius and atrophic lesions of the thymus was most obvious in the immune organs of infected ducks in the DPV CHV₅₀ group, while the lesions were not obvious in the immune organs of the DPV CHV-gI_{N69/78/265A} group.

On the 10th day after injection, compared with DPV CHV₅₀, DPV CHV-gI_{N69/78/265A} showed little or no difference in virus copy number in different tissues, and no death occurred at this time. The low degree of immune organ damage and the inhibition of viral replication are two reasons why the virulence was weakened, and the ducks did not die.

Live attenuated vaccines are highly effective in preventing viral infections. Recently, reverse genetics has been used to modify the viral genome, making it easier to develop these attenuated vaccines quickly. This technique relies on in-depth research on the virus key virulence genes [51]. The genomic sequence of DPV contains many non-essential regions for replication, which can be used as insertion sites for foreign genes. These regions can also act as carriers for multi-recombinant live vaccines [12, 52, 53]. For example, by inserting the P1 and 3C genes of Duck Hepatitis A virus (DHAV) between the US7 and US8 genes of Duck Enteritis Virus (DEV), a recombinant virus (rDEV-US7/US8-P13C) is produced. This recombinant virus triggers the production of neutralising antibodies against both DHAV-3 and DEV in ducks when inoculated. It protects against lethal DEV attacks and completely prevents DHAV-3 infection [54]. The duck Tembusu virus E gene was optimised based on the cloning of the infectious bacterial artificial chromosome (BAC) of the duck enterovirus vaccine pDEV-EF1. The resulting recombinant virus, rDEV-E451-dk, was well expressed in chicken embryo fibroblasts (CEFs) [55]. After inserting multiple *Pseudomonas* outer membrane proteins H (OmpH) between the DEV UL55-LORF11 and UL44-44.5 genes, rDEV-OmpH-UL55 and rDEV-OmpH-UL44 were produced. Specific antibody levels against multiple *Pseudomonas* and DEV were generated after immunisation. This resulted in protection for ducks from the invasion of these two diseases [56]. The results above suggest that viral live vectors can be used not only to express viral immunogens but also to express bacterial immunogens, which can help prevent viral and bacterial

infections. The complete genome of the CHv used in our study as a representative of the DPV potent strain, has been published, and its genetic background is clear [8]. Although the virulence of DPV CHv-gI_{N69/78/265A} in ducks has been reduced, it still maintains some virulence. Figures 6B and 7A show that infected ducks display symptoms such as elevated body temperature and thymus bleeding. After optimising the attenuated strain by mutating other virulence genes, it can be used as a carrier for live vaccines to create multivalent vaccines for controlling DPV and other poultry infections.

The N-glycosylation modification of the gI protein in DPV is crucial for its virulence. In this study, we identified mutant viruses that lack the N-glycosylation site on the gI protein, leading to reduced virulence in ducks. This discovery highlights the importance of N-glycosylation modification of structural proteins in determining the virulence of herpesviruses. The attenuated virus could potentially be further developed as the basis for an avian virus attenuated chimeric live vaccine. This provides a theoretical foundation for investigating the pathogenic mechanism of duck plague virus and developing potential attenuated live vaccines for DPV.

Acknowledgements

This work was supported by grants from National Natural Science Foundation of China (32072894), China Agriculture Research System of MOF and MARA (CARS-42-17) and the Program Sichuan Veterinary Medicine and Drug Innovation Group of China Agricultural Research System (SCCXTD-2020-18).

Authors' contributions

Conceptualisation, YN and AC; methodology, YN software, YN, and QY; validation, MW; formal analysis, YN; investigation, YN; resources, AC, MW, SC, DZ, ML, QY, YW, XZ, SZ, JH, BT, RJ, XO, DS, YY and LZ; data curation, YN; writing-original draft preparation, YN; writing-review and editing, AC; visualisation, BT, RJ, ML, QY, and DS; supervision, YN, and AC; project administration, MW and AC; funding acquisition, MW, AC, RJ, SC, DZ, YH, ZW and ML. All authors read and approved the final manuscript.

Data availability

The datasets used and/or analysed during the current study are available from the corresponding author upon reasonable request.

Declarations

Competing interests

The authors declare that they have no competing interests.

Received: 24 April 2024 Accepted: 26 August 2024

Published online: 26 October 2024

References

- Cheng A (2015) Duck plague. China Agricultural Press, Bei Jing
- Dhama K, Kumar N, Saminathan M, Tiwari R, Karthik K, Kumar MA, Palanivelu P, Shabbir MZ, Malik YS, Singh RK (2017) Duck virus enteritis (duck plague) - a comprehensive update. *Vet Q* 37:57–80
- Cai HQ, Yang X, Yang YY, Feng Y, Wen AL, Yang Y, Wen M, Ou DY (2023) Untargeted metabolomics of the intestinal tract of DEV-infected ducks. *Virol J* 20:305
- Liang ZP, Guo JY, Yuan S, Cheng Q, Zhang XY, Liu Z, Wang CY, Li ZL, Hou B, Huang SJ, Wen F (2022) Pathological and molecular characterization of a duck plague outbreak in southern China in 2021. *Animals (Basel)* 12:3523
- He TQ, Wang MS, Cheng AC, Yang Q, Wu Y, Jia RY, Chen S, Zhu DK, Liu MF, Zhao XX, Zhang SQ, Huang J, Tian B, Ou XM, Mao S, Sun D, Gao Q, Yu YL, Zhang L, Liu YY (2022) Duck plague virus UL41 protein inhibits RIG-I/MDA5-mediated duck IFN- β production via mRNA degradation activity. *Vet Res* 53:22
- Li N, Hong TQ, Li R, Guo MJ, Wang Y, Zhang JZ, Liu JY, Cai YM, Liu SD, Chai TJ, Wei LM (2016) Pathogenicity of duck plague and innate immune responses of the Cherry Valley ducks to duck plague virus. *Sci Rep* 6:32183
- Cheng D, Wu XD, Jia RY, Wang MS, Chen S, Liu MF, Zhu DK, Zhao XX, Wu Y, Yang Q, Zhang SQ, Zhang L, Liu YY, Yin ZQ, Jing B, Cheng AC (2019) CpG oligodeoxynucleotide-specific duck TLR21 mediates activation of NF- κ B signaling pathway and plays an important role in the host defence of DPV infection. *Mol Immunol* 106:87–98
- Wu Y, Cheng AC, Wang MS, Yang Q, Zhu DK, Jia RY, Chen S, Zhou Y, Wang XY, Chen XY (2012) Complete genomic sequence of Chinese virulent duck enteritis virus. *J Virol* 86:5965
- Li CM, Wang MS, Cheng AC, Wu Y, Tian B, Yang Q, Gao Q, Sun D, Zhang SQ, Ou XM, He Y, Huang J, Zhao XX, Chen S, Zhu DK, Liu MF, Jia RY (2023) N-linked glycosylation and expression of duck plague virus pUL10 promoted by pUL49.5. *Microbiol Spectr* 11:e0162523
- Sun KF, Cheng AC, Wang MS (2014) Bioinformatic analysis and characteristics of glycoprotein C encoded by the newly identified UL44 gene of duck plague virus. *Genet Mol Res* 13:4505–4515
- Zhao CK, He TQ, Xu Y, Wang MS, Cheng AC, Zhao XX, Zhu DK, Chen S, Liu MF, Yang Q, Jia RY, Chen XY, Wu Y, Zhang SQ, Liu YY, Yu YL, Zhang L (2019) Molecular characterization and antiapoptotic function analysis of the duck plague virus Us5 gene. *Sci Rep* 9:4851
- Liu T, Wang MS, Cheng AC, Jia RY, Wu Y, Yang Q, Zhu DK, Chen S, Liu MF, Zhao XX, Zhang SQ, Huang J, Mao S, Ou XM, Gao Q, Wen XJ, Sun D, Liu YY, Yu YL, Zhang L, Tian B, Pan LC, Chen XY (2020) Research Note: Duck plague virus glycoprotein I influences cell-cell spread and final envelope acquisition. *Poult Sci* 99:6647–6652
- Wu ZY, Deng JH, Chen MJ, Lu PQ, Yan ZB, Wu XY, Ji QY, Fan HY, Luo YW, Ju CM (2024) Additional insertion of gC gene triggers better immune efficacy of TK/gI/gE-deleted pseudorabies virus in mice. *Viruses* 16:706
- Yu WQ, Liu JY, Liu YN, Forlenza M, Chen HJ (2024) Application of CRISPR/Cas9 for rapid genome editing of pseudorabies virus and bovine herpesvirus-1. *Viruses* 16:311
- Cherepanova N, Shrimal S, Gilmore R (2016) N-linked glycosylation and homeostasis of the endoplasmic reticulum. *Curr Opin Cell Biol* 41:57–65
- Aebi M (2013) N-linked protein glycosylation in the ER. *Biochim Biophys Acta* 1833:2430–2437
- Helenius A, Aebi M (2001) Intracellular functions of N-linked glycans. *Science* 291:2364–2369
- Zhang C, Cai M, Chen SS, Zhang F, Cui TS, Xue ZL, Wang WZ, Zhang BR, Liu XL (2021) The consensus Nglyco-X-S/T motif and a previously unknown Nglyco-N-linked glycosylation are necessary for growth and pathogenicity of *Phytophthora*. *Environ Microbiol* 23:5147–5163
- Lowenthal MS, Davis KS, Formolo T, Kilpatrick LE, Phinney KW (2016) Identification of novel N-glycosylation sites at noncanonical protein consensus motifs. *J Proteome Res* 15:2087–2101
- Xia YQ, Ma ZC, Qiu M, Guo BD, Zhang Q, Jiang HB, Zhang BY, Lin YC, Xuan MR, Sun L, Shu HD, Xiao JH, Ye WW, Wang Y, Wang YM, Dong SM, Tyler BM, Wang YC (2020) N-glycosylation shields *Phytophthora sojae* apoplast effector PsXEG1 from a specific host aspartic protease. *Proc Natl Acad Sci U S A* 117:27685–27693
- Nurdin JA, Kotaki T, Kawagishi T, Sato S, Yamasaki M, Nouda R, Minami S, Kanai Y, Kobayashi T (2023) N-glycosylation of rotavirus NSP4 protein affects viral replication and pathogenesis. *J Virol* 97:e0186122
- Sun SS, Wang QZ, Zhao F, Chen WT, Li Z (2011) Glycosylation site alteration in the evolution of influenza A (H1N1) viruses. *PLoS One* 6:e22844
- Kosik I, Ince WL, Gentles LE, Oler AJ, Kosikova M, Angel M, Magadán JG, Xie H, Brooke CB, Yewdell JW (2018) Influenza A virus hemagglutinin glycosylation compensates for antibody escape fitness costs. *PLoS Pathog* 14:e1006796

24. Huang Y, Owino SO, Crevar CJ, Carter DM, Ross TM (2020) N-linked glycans and K147 residue on hemagglutinin synergize to elicit broadly reactive H1N1 influenza virus antibodies. *J Virol* 94:e01432-19
25. Riera E, Pérez-Núñez D, García-Belmonte R, Miorin L, García-Sastre A, Revilla Y (2021) African swine fever virus induces STAT1 and STAT2 degradation to counteract IFN-I signaling. *Front Microbiol* 12:722952
26. García-Belmonte R, Pérez-Núñez D, Pittau M, Richt JA, Revilla Y (2019) African swine fever virus Armenia/07 virulent strain controls interferon beta production through the cGAS-STING pathway. *J Virol* 93:e02298-18
27. Watanabe Y, Bowden TA, Wilson IA, Crispin M (2019) Exploitation of glycosylation in enveloped virus pathobiology. *Biochim Biophys Acta Gen Subj* 1863:1480–1497
28. Fukui A, Maruzuru Y, Takeshima K, Koyanagi N, Kato A, Kawaguchi Y (2023) Establishment of a system to quantify wild-type herpes simplex virus-induced cell-cell fusion reveals a role of N-glycosylation of HSV-1 envelope glycoprotein B in cell-cell fusion. *Microbiol Immunol* 67:114–119
29. Herman X, Far J, Peeters M, Quinton L, Chaumont F, Navarre C (2023) In vivo deglycosylation of recombinant glycoproteins in tobacco BY-2 cells. *Plant Biotechnol J* 21:1773–1784
30. Chen J, Schaller S, Jardtzyk TS, Longnecker R (2020) Epstein-Barr virus gH/gL and Kaposi's sarcoma-associated herpesvirus gH/gL bind to different sites on EphA2 to trigger fusion. *J Virol* 94:e01454-20
31. You Y, Liu T, Wang MS, Cheng AC, Jia RY, Yang Q, Wu Y, Zhu DK, Chen S, Liu MF, Zhao XX, Zhang SQ, Liu YY, Yu YL, Zhang L (2018) Duck plague virus Glycoprotein J is functional but slightly impaired in viral replication and cell-to-cell spread. *Sci Rep* 8:4069
32. Shen BJ, Ruan PL, Cheng AC, Wang MS, Zhang W, Wu Y, Yang Q, Tian B, Ou XM, Mao S, Sun D, Zhang SQ, Zhu DK, Jia RY, Chen S, Liu MF, Zhao XX, Huang J, Gao Q, Yu YL, Zhang L, Pan LC (2023) Characterization of a unique novel LORF3 protein of duck plague virus and its potential pathogenesis. *J Virol* 97:e0157722
33. Wang J, Wu K, Ni LQ, Li CX, Peng RY, Li Y, Fan ZJ, Yin FF, Deng F, Shen S, Wu XL (2023) Effects of US7 and UL56 on cell-to-cell spread of human herpes simplex virus 1. *Viruses* 15:2256
34. Balan P, Davis-Poynter N, Bell S, Atkinson H, Browne H, Minson T (1994) An analysis of the in vitro and in vivo phenotypes of mutants of herpes simplex virus type 1 lacking glycoproteins gG, gE, gI or the putative gJ. *J Gen Virol* 75:1245–1258
35. Park A, Ra EA, Lee TA, Choi HJ, Lee E, Kang SJ, Seo JY, Lee S, Park B (2019) HCMV-encoded US7 and US8 act as antagonists of innate immunity by distinctively targeting TLR-signaling pathways. *Nat Commun* 10:4670
36. Zhao M, Ma GQ, Yan XX, Li XH, Wang E, Xu XX, Zhao JB, Ma XL, Zeng JX (2024) Microbial infection promotes amyloid pathology in a mouse model of Alzheimer's disease via modulating γ -secretase. *Mol Psychiatry* 29:1491–1500
37. Yin H, Li ZJ, Zhang JK, Huang JP, Kang HT, Tian J, Qu LD (2020) Construction of a US7/US8/UL23/US3-deleted recombinant pseudorabies virus and evaluation of its pathogenicity in dogs. *Vet Microbiol* 240:108543
38. Delva JL, Van Waesberghe C, Van Den Broeck W, Lamote JA, Verecke N, Theuns S, Couck L, Favoreel HW (2022) The attenuated pseudorabies virus vaccine strain bartha hyperactivates plasmacytoid dendritic cells by generating large amounts of cell-free virus in infected epithelial cells. *J Virol* 96:e0219921
39. Scherer J, Hogue IB, Yaffe ZA, Tanneti NS, Winer BY, Vershinin M, Enquist LW (2020) A kinesin-3 recruitment complex facilitates axonal sorting of enveloped alpha herpesvirus capsids. *PLoS Pathog* 16:e1007985
40. Vallbracht M, Klupp BG, Mettenleiter TC (2021) Influence of N-glycosylation on expression and function of pseudorabies virus glycoprotein gB. *Pathogens* 10:61
41. Oliver SL, Xing Y, Chen DH, Roh SH, Pintilie GD, Bushnell DA, Sommer MH, Yang E, Carfi A, Chiu W, Arvin AM (2020) A glycoprotein B-neutralizing antibody structure at 2.8 Å uncovers a critical domain for herpesvirus fusion initiation. *Nat Commun* 11:4141
42. Großkopf AK, Ensser A, Neipel F, Jungnickl D, Schlagowski S, Desrosiers RC, Hahn AS (2018) A conserved Eph family receptor-binding motif on the gH/gL complex of Kaposi's sarcoma-associated herpesvirus and rhesus monkey rhadinovirus. *PLoS Pathog* 14:e1006912
43. Aksnes I, Markussen T, Braeen S, Rimstad E (2020) Mutation of N-glycosylation sites in Salmonid Alphavirus (SAV) Envelope proteins attenuate the virus in cell culture. *Viruses* 12:1071
44. Zhang SZ, Wang XL, He Y, Hu T, Guo JQ, Wang MS, Jia RY, Zhu DK, Liu MF, Zhao XX, Yang Q, Wu Y, Zhang SQ, Huang J, Mao S, Ou XM, Gao Q, Sun D, Liu YY, Zhang L, Chen S, Cheng AC (2021) N130, N175 and N207 are N-linked glycosylation sites of duck Tembusu virus NS1 that are important for viral multiplication, viremia and virulence in ducklings. *Vet Microbiol* 261:109215
45. Marín-Menguiano M, Moreno-Sánchez I, Barrales RR, Fernández-Álvarez A, Ibeas JI (2019) N-glycosylation of the protein disulfide isomerase Pdi1 ensures full *Ustilago maydis* virulence. *PLoS Pathog* 15:e1007687
46. Fernández-Álvarez A, Elías-Villalobos A, Ibeas JI (2009) The O-mannosyltransferase PMT4 is essential for normal appressorium formation and penetration in *Ustilago maydis*. *Plant Cell* 21:3397–3412
47. Mei J, Li ZQ, Zhou SQ, Chen XL, Wilson RA, Liu WD (2023) Effector secretion and stability in the maize anthracnose pathogen *Colletotrichum graminicola* requires N-linked protein glycosylation and the ER chaperone pathway. *New Phytol* 240:1449–1466
48. Doms RW, Lamb RA, Rose JK, Helenius A (1993) Folding and assembly of viral membrane proteins. *Virology* 193:545–562
49. Bagdonaite I, Wandall HH (2018) Global aspects of viral glycosylation. *Glycobiology* 28:443–467
50. Ruan PL, Feng X, Cheng AC, Wang MS, Zhang W, Wu Y, Yang Q, Tian B, Ou XM, Sun D, Zhang SQ, Mao S, Zhu DK, Jia RY, Chen S, Liu MF, Zhao XX, Huang J, Gao Q, Yu YL, Zhang L, Pan LC (2022) Evaluation of safety and immunogenicity of duck-plague virus gC/gE double gene deletion. *Front Immunol* 13:963009
51. Fang EY, Li M, Liu XH, Hu KX, Liu LJ, Zhang ZL, Li XX, Peng QH, Li YH (2023) NS1 protein N-linked glycosylation site affects the virulence and pathogenesis of Dengue virus. *Vaccines (Basel)* 11:959
52. Liu T, Wang MS, Cheng AC, Jia RY, Yang Q, Wu Y, Liu MF, Zhao XX, Chen S, Zhang SQ, Zhu DK, Tian B, Rehman MU, Liu YY, Yu YL, Zhang L, Pan LC, Chen XY (2020) Duck plague virus gE serves essential functions during the virion final envelopment through influence capsids budding into the cytoplasmic vesicles. *Sci Rep* 10:5658
53. Wu Y, Li YG, Wang MS, Sun KF, Jia RY, Chen S, Zhu DK, Liu MF, Yang Q, Zhao XX, Chen XY, Cheng AC (2017) Preliminary study of the UL55 gene based on infectious Chinese virulent duck enteritis virus bacterial artificial chromosome clone. *Virology* 14:78
54. Yang FC, Liu P, Li XH, Liu R, Gao L, Cui HY, Zhang YP, Liu CJ, Qi XL, Pan Q, Liu AJ, Wang XM, Gao YL, Li K (2021) Recombinant duck enteritis virus-vectored bivalent vaccine effectively protects against duck hepatitis A virus infection in ducks. *Front Microbiol* 12:813010
55. Chen L, Yu B, Hua JG, Ni Z, Ye WC, Yun T, Zhang C (2019) Optimized expression of duck Tembusu virus E gene delivered by a vectored duck enteritis virus in vitro. *Mol Biotechnol* 61:783–790
56. Apinda N, Muenthaisong A, Chomjit P, Sangkakam K, Namboopha B, Rittipornlertrak A, Koonyosying P, Yao YX, Nair V, Sthitmatee N (2022) Simultaneous protective immune responses of ducks against duck plague and fowl cholera by recombinant duck enteritis virus vector expressing *Pasteurella multocida* OmpH gene. *Vaccines (Basel)* 10:1358

Publisher's Note

Springer Nature remains neutral with regard to jurisdictional claims in published maps and institutional affiliations.